

# Hessian Eigenfunctions for Triangular Mesh Parameterization

Daniel Mejia, Oscar Ruiz-Salguero and Carlos A. Cadavid

Laboratorio de CAD CAM CAE, Universidad EAFIT, Cra 49 No-7 Sur-50, 050022, Medellin, Colombia

**Keywords:** Applied Differential Geometry, Dimensionality Reduction, Hessian Locally Linear Embedding, Manifold Learning, Mesh Parameterization.

**Abstract:** Hessian Locally Linear Embedding (HLLLE) is an algorithm that computes the nullspace of a Hessian functional  $\mathcal{H}$  for Dimensionality Reduction (DR) of a sampled manifold  $M$ . This article presents a variation of classic HLLLE for parameterization of 3D triangular meshes. Contrary to classic HLLLE which estimates local Hessian nullspaces, the proposed approach follows intuitive ideas from Differential Geometry where the local Hessian is estimated by quadratic interpolation and a partition of unity is used to join all neighborhoods. In addition, local average triangle normals are used to estimate the tangent plane  $T_x M$  at  $x \in M$  instead of PCA, resulting in local parameterizations which reflect better the geometry of the surface and perform better when the mesh presents sharp features. A high frequency dataset (*Brain*) is used to test our algorithm resulting in a higher rate of success (96.63%) compared to classic HLLLE (76.4%).

## 1 INTRODUCTION

Dimensionality Reduction (DR) takes a  $d$ -manifold  $M \subset \mathbb{R}^D$  and computes a map  $\mathbf{h} : M \rightarrow \mathbb{R}^d$  such that: 1)  $\mathbf{h}$  is bijective and 2)  $\mathbf{h}$  and  $\mathbf{h}^{-1}$  are continuous. Therefore,  $\mathbf{h}$  is an homeomorphism and the image of  $M$  under  $\mathbf{h}$  is a DR of  $M$ .

Mesh Parameterization can be seen as a particular case of DR where  $M \subset \mathbb{R}^3$  is a triangular mesh of a 2-manifold (i.e.  $D = 3$  and  $d = 2$ ). Triangular meshes are very common data structures in CAD CAM CAE applications and parameterization of such meshes is relevant for areas such as: reverse engineering, tool path planning, feature detection, etc.

A natural way to handle Mesh Parameterization is to attack the problem from the point of view of DR. Classic HLLLE (Hessian Locally Linear Embedding) (Donoho and Grimes, 2003) is an algorithm which proposes to compute a DR of  $M$  by computing the eigenvectors of a Hessian functional. This article proposes a modification for the classic HLLLE which can be applied to triangular meshes. Our proposed approach computes a partition of unity on  $M$  and estimates the tangent Hessian on each neighborhood  $N_i$  of  $M$  by interpolating any function  $f$  with second degree polynomials. In addition, local average triangle normals are used to compute the tangent local plane  $T_x M$  of  $M$  which is more consistent than Principal Component Analysis (PCA) specially for surfaces with sharp features.

The remainder of this article is organized as follows: Section 2 reviews the relevant literature. Section 3 describes the implemented methodology. Section 4 discusses and compares the results of the proposed approach against classic HLLLE. Section 5 concludes the paper and introduces what remains for future work.

## 2 LITERATURE REVIEW

Given a set of points  $X = [x_1, x_2, \dots, x_n] \subset \mathbb{R}^D$  lying on a  $d$ -manifold  $M$ , DR seeks a homeomorphic function  $\mathbf{h} : M \rightarrow \mathbb{R}^d$  such that the set of points  $[\mathbf{h}(x_1), \mathbf{h}(x_2), \dots, \mathbf{h}(x_n)] \subset \mathbb{R}^d$  compose a DR of  $X$ . For the rest of the article we assume  $D = 3$  and  $d = 2$ , turning the DR problem into a Mesh Parameterization one.

The most popular algorithm for DR is the Principal Component Analysis (PCA). PCA is a linear algorithm which parameterizes  $M$  by projecting  $X$  onto a plane, which is only a valid parameterization if  $\mathbf{h}$  is linear. However, this assumption limits the algorithm making it useful only for trivial cases.

For nonlinear manifolds, other approaches have been proposed in the literature. For example, Isomap (Tenenbaum et al., 2000) attempts to compute an isometric parameterization of  $M$  by computing the geodesic distances in  $M$  and reproducing them in the

parameter space. Isomap has been successfully applied in the context of Mesh Parameterization (Sun and Hancock, 2008; Ruiz et al., 2015). Usually a shortest path algorithm such as Dijkstra's or Floyd's is used to estimate geodesic distances which fail for non-convex manifolds such as surfaces with holes.

Spectral theory is an important branch of graph theory where several DR algorithms have been derived. Laplacian Eigenmaps (Belkin and Niyogi, 2003) computes the Laplacian matrix which acts over any function defined on the graph of  $M$  measuring its curvature. Diffusion Maps (DM) (Lafon and Lee, 2006) computes the Markov matrix which estimates the transition probability between vertices of the graph of  $M$ . DR is achieved in both cases by computing the eigenvectors of these matrices respectively. Spectral algorithms preserve topologic properties of the underlying graph keeping adjacent points near in the parameter space. However, these algorithms usually fail to preserve geometric properties which becomes important in Mesh Parameterization applications.

Other DR algorithms focus on a more local approach where each neighborhood is first parameterized locally and then all the neighborhoods are aligned in the parameter space trying to preserve geometric properties. Locally Linear Embedding (LLE) (Roweis and Saul, 2000) expresses each point in  $M$  as a linear combination of its neighbors and then computes the DR attempting to preserve such structure in the parameter space for all the points. Similarly, Local Tangent Space Alignment (LTSA) (Zhang and Zha, 2002) projects each neighborhood onto the tangent plane via PCA and then attempts to align all the neighborhoods in the parameter space using rigid transformations. These algorithms highly preserve geometric properties and perform well for non-convex manifolds. However, they expect that each neighborhood lies on a linear subspace which fails at sharp features of 3D meshes resulting in non-bijective parameterizations. Most Mesh Parameterization algorithms also follow this idea by aligning triangles in the parameter space preserving geometric properties for each triangle (Lévy et al., 2002; Liu et al., 2008; Athanasiadis et al., 2013; Smith and Schaefer, 2015) or as LLE does, by locally convex linear combinations (Floater, 1997; Lee et al., 2002). Other Mesh Parameterization algorithms compute the resulting parameterization in terms of the angles of the Mesh (Sheffer and de Sturler, 2001; Kharevych et al., 2006; Zayer et al., 2007).

## 2.1 Classic Hessian Locally Linear Embedding (HLLE)

Classic Hessian Locally Linear Embedding (Donoho and Grimes, 2003) is a DR algorithm which combines ideas from LLE and LTSA with ideas from discrete differential geometry. HLLE computes a local parameterization of each neighborhood using PCA. But instead of aligning all neighborhoods by a rigid mapping, HLLE estimates a Hessian functional  $\mathcal{H}$  on  $M$  (similar to Laplacian Eigenmaps which estimates a Laplacian functional) and computes the DR of  $M$  by estimating the kernel of  $\mathcal{H}$ , i.e.  $\ker(\mathcal{H}) = \{f | \mathcal{H}f = 0\}$ .

In order to compute  $\mathcal{H}$ , the tangent Hessian  $\mathbf{H}_x^{\tan}$  must be defined (Donoho and Grimes, 2003):

$$\mathbf{H}_x^{\tan} f = \begin{bmatrix} \frac{\partial^2 f}{\partial b_1^2} & \frac{\partial^2 f}{\partial b_1 \partial b_2} \\ \frac{\partial^2 f}{\partial b_2 \partial b_1} & \frac{\partial^2 f}{\partial b_2^2} \end{bmatrix}, \quad (1)$$

where  $b_1, b_2 \in \mathbb{R}^3$  is an orthonormal basis for the tangent plane  $T_x M$  at  $x$ . If  $\mathbf{f} = \{f_1, f_2, \dots, f_n\}$  with  $f_i = f(x_i)$  is the function  $f$  restricted to the set of points  $X$ , then the Hessian functional  $\mathcal{H}$  is defined as (Donoho and Grimes, 2003):

$$\mathcal{H}f = \int_M \|\mathbf{H}_x^{\tan} f\|_F^2 dA = \sum_{i=1}^n \int_{M_i} \phi_i \|\mathbf{H}_x^{\tan} f\|_F^2 dA \approx \mathbf{f}^T \mathbf{K} \mathbf{f} \quad (2)$$

where  $f \in \mathcal{C}^2(M)$  is a smooth function defined on  $M$ ,  $\|\cdot\|_F$  is the Frobenius norm,  $dA$  is a surface differential,  $(M_i, \phi_i)$  is a partition of unity of  $M$  and  $\mathbf{K} = (\mathbf{K}_1 + \mathbf{K}_2, \dots, \mathbf{K}_n)$  is the discrete Hessian estimator computed by adding each local Hessian estimator  $\mathbf{K}_i$  at each neighborhood  $N_i$ .

Since the matrix  $\mathbf{K}$  approximates the Hessian functional on  $M$ , the kernel of  $\mathcal{H}$  can be estimated by solving the following minimization problem (Donoho and Grimes, 2003):

$$\begin{aligned} \mathbf{h}_1 &= \arg \min_{\mathbf{f}} \mathbf{f}^T \mathbf{K} \mathbf{f}, & \mathbf{h}_2 &= \arg \min_{\mathbf{f}} \mathbf{f}^T \mathbf{K} \mathbf{f} \\ \text{s.t.} & & & \\ \|\mathbf{h}_i\| &= 1, & \mathbf{h}_i &\perp \mathbf{1}, & \mathbf{h}_1 &\perp \mathbf{h}_2, \\ & & i &= 1, 2 \end{aligned} \quad (3)$$

where  $\mathbf{h}_1 = [h_1(x_1), \dots, h_1(x_n)]^T$  and  $\mathbf{h}_2 = [h_2(x_1), \dots, h_2(x_n)]^T$  are the respective coordinates of  $X$  in the parameter space. The constant function  $f(x) = c$ ,  $c \in \mathbb{R}$ , is in the kernel of  $\mathcal{H}$  (the Hessian of any constant function is 0 as per eq. (1)). Therefore, the constraint  $\mathbf{h}_i \perp \mathbf{1}$  avoids collapsing all the vertices to a single point. The constraint

$\mathbf{h}_1 \perp \mathbf{h}_2$  guarantees linear independence which avoids collapsing the surface into a line. The constraint  $\|\mathbf{h}_i\| = 1$  fixes the scale of the solution.

Eq. (3) can be solved by computing the eigenvectors of  $\mathbf{K}$  associated to the second and third lowest eigenvalue (the eigenvector associated to the lowest eigenvalue corresponds to the constant function  $\mathbf{1}$ ).

Basically, classic HLLE algorithm consists of: 1) estimate the local Hessian functionals  $\mathbf{K}_1, \mathbf{K}_2, \dots, \mathbf{K}_n$  and the Hessian functional  $\mathbf{K} = \mathbf{K}_1 + \mathbf{K}_2 + \dots + \mathbf{K}_n$  and 2) compute the eigenvectors of  $\mathbf{K}$  with the smallest eigenvalue (Donoho and Grimes, 2003).

Like LLE and LTSA, classic HLLE may present problems for datasets with sharp features resulting in non-bijective mappings. In addition, the computation of the matrix  $\mathbf{K}_i$  which estimates the local Hessian functional  $\mathcal{H}|_i$  is not consistent with the definition in eq. (2) as only Hessian nullspaces are computed.

**Conclusions of the Literature Review.** In Mesh Parameterization applications, the preservation of geometric properties is a priority over topology preservation. Algorithms such as Laplacian Eigenmaps and DM present highly distorted parameterizations. Therefore, algorithms that preserve geometric properties such as Isomap, LLE, LTSA and classic HLLE are more effective. However, these algorithms present drawbacks such as the inability to work with convex datasets or high frequency datasets, which are very common in engineering applications. Mesh Parameterization algorithms do not face such problems. However they are only restricted to triangular meshes.

To partially overcome these problems, this article proposes a variation of the classic HLLE algorithm for parameterization of triangular meshes. Classic HLLE algorithm is selected for this purpose since such algorithm has provided better experimental results for Mesh Parameterization than other DR algorithms (Ruiz et al., 2015). Also, since HLLE is a DR algorithm, the proposed approach can be easily extended to meshes composed of non-triangular faces posing a potential advantage over traditional Mesh Parameterization algorithms.

### 3 METHODOLOGY

In order to parameterize  $M$ , we propose to follow the same idea of the classic HLLE which is described in section 2.1 (Donoho and Grimes, 2003): 1) estimate the tangent Hessian  $\mathbf{H}_x^{\tan}$  and the Hessian functional  $\mathbf{K}_i$  at each  $N_i$ , 2) estimate the Hessian functional  $\mathcal{H}$  on  $M$  as per eq. (2) and 3) estimate the kernel of  $\mathcal{H}$  for

Mesh Parameterization via eigendecomposition. The algorithm is briefly described below:

1. For each neighborhood estimate the tangent plane  $T_x M$  at  $x_i$  by computing the local average normal vector  $\bar{n}_i$  and compute a local parameterization  $O_i$  by projecting  $N_i$  onto  $T_x M$ .
2. Estimate the tangent Hessian  $\mathbf{H}_x^{\tan} f$  and  $\|\mathbf{H}_x^{\tan} f\|_{\mathbb{F}}^2$  at  $x_i$  by quadratic interpolation.
3. Apply the partition of unity  $\phi_i$  to estimate the local Hessian functional  $\int_{M_i} \phi_i \|\mathbf{H}_x^{\tan}\|_{\mathbb{F}}^2 dA \approx \mathbf{f}^T \mathbf{K}_i \mathbf{f}$ .
4. Estimate the global Hessian functional  $\mathcal{H} \approx \mathbf{K} = \sum_{i=1}^n \mathbf{K}_i$ .
5. Compute two orthogonal functions  $\mathbf{h}_1$  and  $\mathbf{h}_2$  which solve the optimization problem posed in eq. (3) by eigendecomposition of the matrix  $\mathbf{K}$ .

The steps of the algorithm are detailed below.

#### 3.1 Tangent Plane $T_x M$ and Local Parameterization $O_i$

In order to estimate the tangent Hessian  $\mathbf{H}_x^{\tan}$  at  $x_i$ , the tangent plane  $T_x M$  at  $x_i$  is estimated. Classic HLLE estimates  $T_x M$  applying PCA on  $N_i$ . However, we propose to estimate  $T_x M$  using the information of the triangulation  $T$  as follows: let  $\{t_{i_1}, t_{i_2}, \dots\}$  and  $\{n_{i_1}, n_{i_2}, \dots\}$  be the set of triangles adjacent to  $x_i$  and their corresponding normal vectors respectively. Set  $T_x M$  as the plane with origin  $x_i$  and normal  $\bar{n}_i$  (where  $\bar{n}_i$  is the average of  $\{n_{i_1}, n_{i_2}, \dots\}$ ). Finally,  $O_i$  is computed by projecting  $N_i$  onto  $T_x M$ .

Using the local average adjacent normals to compute  $T_x M$  usually results in better approximations of the tangent plane than PCA and if  $N_i$  belongs to a sharp region, PCA may fail to recover a bijective parameterization while the local average normals parameterization has a better chance of being bijective. These local parameterizations affect the resulting global parameterization in the sense that local non-bijectivity results in a folding of the surface in the global parameterization.

#### 3.2 Tangent Hessian $\mathbf{H}_x^{\tan} f$ and

$$\|\mathbf{H}_x^{\tan} f\|_{\mathbb{F}}^2$$

The definition of tangent Hessian in eq. (1) requires a smooth function defined on  $M$ . Quadratic interpolation is used in order to estimate such Hessian in a discrete surface. Let  $[b_1, b_2]$  be an orthonormal basis of  $T_x M$  at  $x_i$ . Therefore, any point  $p$  on  $T_x M$  at  $x_i$  can be expressed as  $p = ub_1 + vb_2 + x_i$ . Let  $\{u_{i_1}, u_{i_2}, \dots, u_{i_k}\}$  and  $\{v_{i_1}, v_{i_2}, \dots, v_{i_k}\}$  be the corresponding coordinates of  $O_i$  in this basis. If  $\mathbf{f}_i =$

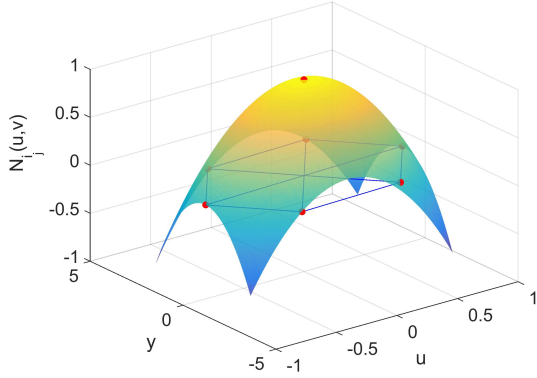


Figure 1: Quadratic interpolation function  $\mathbb{N}_{ij}$  at  $N_i$  such that  $\mathbb{N}_{ij}(x_{i_k}) = 1$  if  $j = k$ , 0 otherwise.

$\{f_{i_1}, f_{i_2}, \dots, f_{i_k}\}$  are the values of  $f$  restricted to  $N_i$ , then  $f$  can be interpolated at  $T_x M$  by a second order polynomial as follows:

$$f(u, v) = \sum_{j=1}^k \mathbb{N}_{ij}(u, v) f_{i_j}, \quad (4)$$

with  $\mathbb{N}_{ij}(u, v) = \alpha_j u^2 + \beta_j uv + \gamma_j v^2 + \delta_j u + \varepsilon_j v + \zeta_j$ . Since  $f(u_j, v_j) = f_{i_j}$ , the interpolation functions  $\mathbb{N}_{ij}$  are required to satisfy  $\mathbb{N}_{ij}(u_{i_l}, v_{i_l}) = 1$  if  $j = l$  and  $\mathbb{N}_{ij}(u_{i_l}, v_{i_l}) = 0$  if  $j \neq l$  (fig. 1). The coefficients of  $\mathbb{N}_{ij}$  are computed by solving the arising linear system of equations in a least squares sense. Afterwards, equation (1) can be approximated as:

$$\mathbf{H}_x^{\tan} f \approx \begin{bmatrix} 2\boldsymbol{\alpha}_i^T \mathbf{f}_i & \boldsymbol{\beta}_i^T \mathbf{f}_i \\ \boldsymbol{\beta}_i^T \mathbf{f}_i & 2\boldsymbol{\gamma}_i^T \mathbf{f}_i \end{bmatrix}, \quad (5)$$

where  $\boldsymbol{\alpha}_i$ ,  $\boldsymbol{\beta}_i$  and  $\boldsymbol{\gamma}_i$  are column vectors with the corresponding coefficients of the quadratic terms in eq. (4). Therefore, the norm of the tangent Hessian can be estimated as  $\|\mathbf{H}_x^{\tan} f\|_F^2 \approx \mathbf{f}_i^T \mathbf{C}_i \mathbf{f}_i$ , where  $\mathbf{C}_i$  is a symmetric matrix defined as:

$$\mathbf{C}_i = 4\boldsymbol{\alpha}_i \boldsymbol{\alpha}_i^T + 2\boldsymbol{\beta}_i \boldsymbol{\beta}_i^T + 4\boldsymbol{\gamma}_i \boldsymbol{\gamma}_i^T \quad (6)$$

### 3.3 Partition of Unity $\phi$ and Local Hessian Functional $\mathbf{K}_i$

Eq. (2) requires a partition of unity  $(M_i, \phi_i)$  defined on  $M$ . A partition of unity  $\boldsymbol{\phi} = \{\phi_1, \phi_2, \dots, \phi_n\}$  is a set of functions satisfying the following properties:

1.  $M_i$  is an open subset of  $M$ .
2.  $\bigcup_{i=1}^n M_i = M$ .
3.  $\phi_i : M \rightarrow [0, 1]$ .
4.  $\phi_i(x) = 0$  if  $x \notin M_i$ .

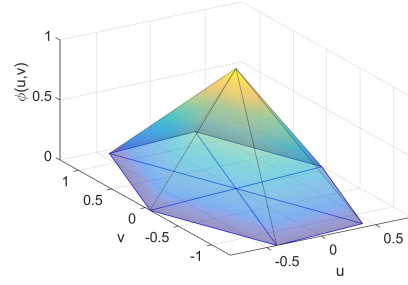


Figure 2: Partition of unity  $\phi_i$  for a selected neighborhood  $N_i$ .  $\phi_i$  equals to 1 at  $x_i$  and vanishes to 0 at adjacent points.

5.  $\sum_{i=1}^n \phi_i(x) = 1$  for all  $x \in M$ .

A partition of unity for  $M$  can be build as a set of piecewise linear functions such that for  $N_i$ ,  $\phi_i$  is defined as:

$$\phi_i(x_j) = \begin{cases} 1 & \text{if } i = j \\ 0 & \text{otherwise} \end{cases}, \quad \forall j = 1, 2, \dots, n. \quad (7)$$

By its definition in eq. (7),  $\phi_i$  vanishes at other neighborhoods. Therefore:

$$\int_M \phi_i dA = \int_{M_i} \phi_i dA = \frac{1}{3} \sum_j A_{ij}, \quad (8)$$

where  $A_{ij}$  is the area of the  $j$ -th adjacent triangle of  $x_i$ . It is not hard to check that eq. (7) satisfies the properties of a partition of unity if  $M$  is a triangular mesh.

Finally, from eqs. (6) and (8) the local Hessian functional in eq. (2) can be estimated:

$$\begin{aligned} \int_{M_i} \phi_i \|\mathbf{H}_x^{\tan} f\|_F^2 dA &\approx \left( \int_{M_i} \phi_i dA \right) \mathbf{f}_i^T \mathbf{C}_i \mathbf{f}_i \\ &= \left( \frac{1}{3} \sum_j A_{ij} \right) \mathbf{f}_i^T \mathbf{C}_i \mathbf{f}_i. \end{aligned} \quad (9)$$

The matrix  $(\frac{1}{3} \sum_j A_{ij}) \mathbf{C}_i$  estimates the local Hessian functional for any  $\mathbf{f}_i$ . Therefore, the matrix  $\mathbf{K}_i$  is built as an  $n \times n$  symmetric matrix which has the terms of  $(\frac{1}{3} \sum_j A_{ij}) \mathbf{C}_i$  at the indices dictated by  $(N_i, N_i)$ , and zeros elsewhere.

### 3.4 Global Hessian $\mathcal{H}$ and Parameterization of $M$

The Hessian functional is estimated exactly as described in (Donoho and Grimes, 2003) by adding each local Hessian:  $\mathcal{H} \approx \mathbf{K} = \sum_i \mathbf{K}_i$ . Finally, the parameterization  $\mathbf{h}_1, \mathbf{h}_2$  of  $M$  is achieved by solving the minimization problem in eq. (3) via eigendecomposition of the matrix  $\mathbf{K}$ .

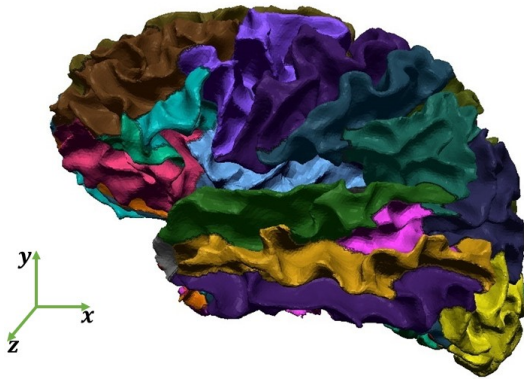


Figure 3: Segmented *Brain* dataset.

## 4 RESULTS AND DISCUSSION

In this section we present and discuss the parameterization results obtained for the segmented *Brain* dataset (Desikan et al., 2006) and the *Face* dataset (Ruiz et al., 2015). We also present an asymptotic time complexity comparison for our algorithm and several Mesh Parameterization algorithms.

### 4.1 Datasets

The *Brain* dataset (fig. 3) presents several challenges in terms of Mesh Parameterization given the high curvatures and the low developability of the surface. We remeshed all the sub-meshes and some of them were also partitioned manually prior to parameterization. From the 89 sub-meshes, classic HLLE computed only 68 (76.40%) bijective parameterizations while our algorithm computed 86 (96.63%) bijective mappings.

The *Left Hemisphere - Frontal Pole* sub-mesh (fig. 4) presents a high frequency zone near a corner. Fig. 5 presents the parameterization results obtained by clas-

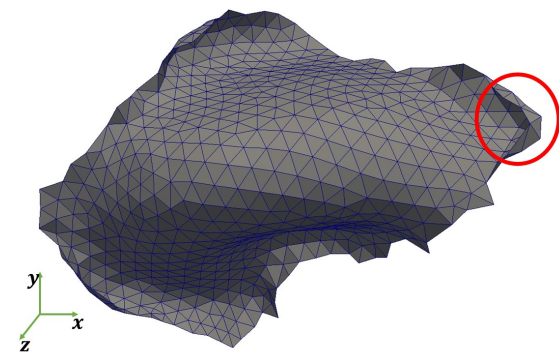


Figure 4: *Left Hemisphere - Frontal Pole* mesh. The red ellipse marks a high frequency zone.

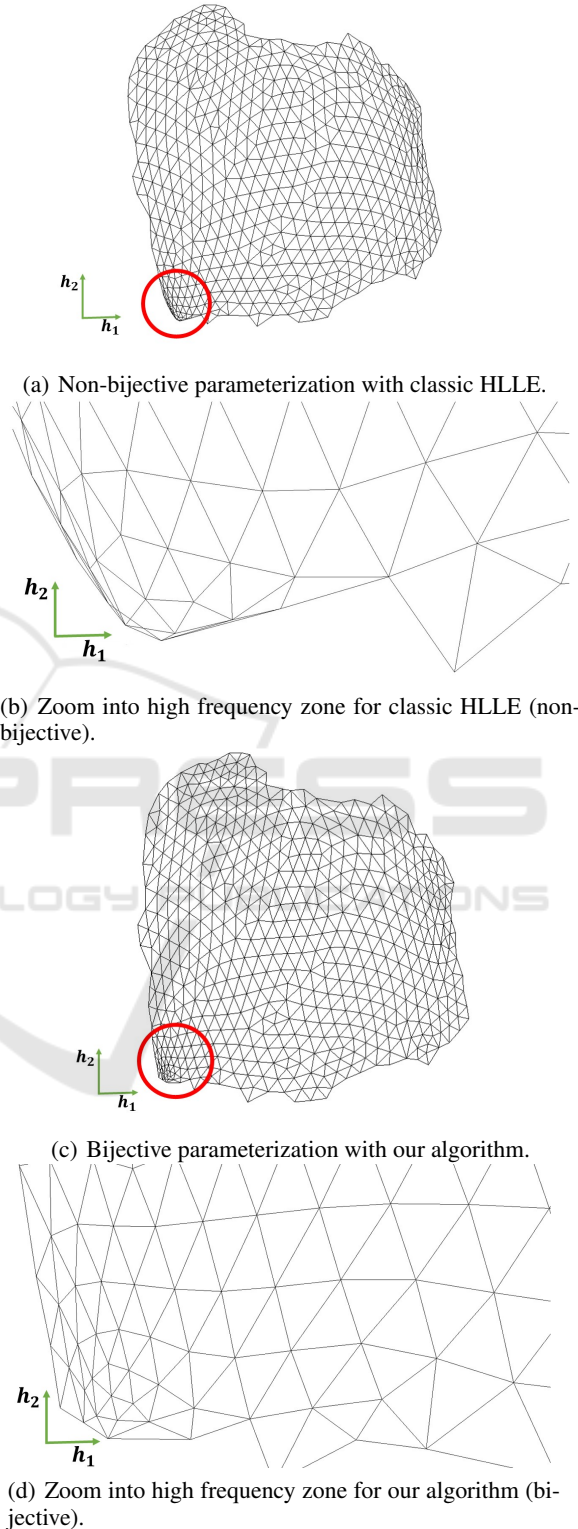
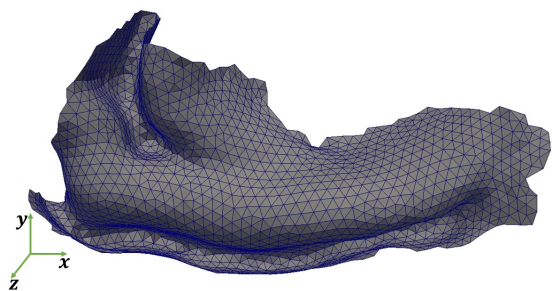
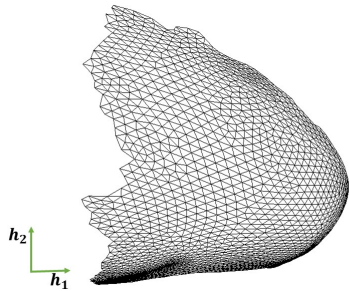


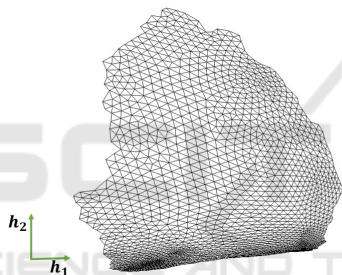
Figure 5: Parameterization results for the *Left Hemisphere - Frontal Pole* mesh. The red ellipse marks the high frequency zone.



(a) Left Hemisphere - Rostral Anterior Cingulate mesh.



(b) Non-bijective parameterization with classic HLLLE.



(c) Bijective parameterization with our algorithm.

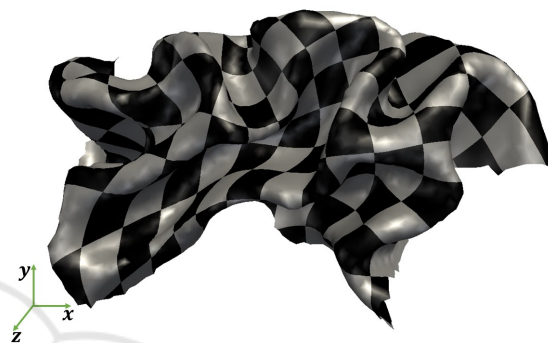
Figure 6: Parameterization results for the *Left Hemisphere - Rostral Anterior Cingulate* mesh with classic HLLLE and our algorithm.

sic HLLLE and our algorithm. As described in section 3.1 Classic HLLLE parameterization (fig. 5(a)) computes local non-bijective parameterizations at such sharp zone. As a consequence, the parameterized surface folds as detailed in fig. 5(b) resulting in a non-bijective parameterization. On the other hand, our algorithm does not face this problem and correctly unfolds the surface recovering a bijective parameterization (figs. 5(c) and 5(d)).

Fig. 6 presents the parameterization results for the *Right Hemisphere - Temporal Pole* sub-mesh which presents several sharp sections (fig. 6(a)) using the classic HLLLE algorithm and our algorithm. Classic HLLLE fails to adequately parameterize some local features of the surface resulting in a non-bijective mapping (fig. 6(b)). Again, our algorithm does not face this problem resulting in a bijective mapping (fig. 6(c)). In addition, less shape distortion can be evi-



(a) Left Hemisphere - Rostral Middle Frontal texture map.



(b) Right Hemisphere - Lateral Occipital bijective texture map.

Figure 7: Texture map of other bijective mappings from the *Brain* dataset computed with our algorithm.

denced from our algorithm compared to classic HLLLE parameterization (figs. 6(b) and 6(c)) due to the explicit computation of the local Hessian functional.

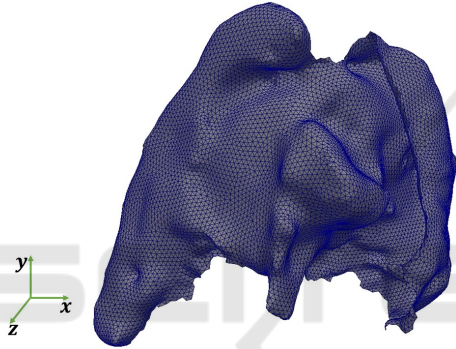
Results of our algorithm for other sub-meshes of the *Brain* are presented in fig. 7. The texture map of a chessboard pattern illustrates the angular distortion of the respective parameterization where less local distortion is present if the corners of the mapped rectangles are near 90 degrees. All the four parameterizations are bijective despite the high frequencies of the sub-meshes.

Highly non-developable meshes still pose a problem to our algorithm. Fig. 8 presents a case of the *Brain* dataset where the algorithm fails to recover a bijective parameterization. In this case the parameterization degenerates near the boundary (i.e. triangles overlap) in the parameter space due to the high non-developability of such zones in the surface.

Finally, fig. 9 presents the texture map (computed by our algorithm) of a chessboard pattern onto the *Face* dataset. The underlying parameterization is bijective, handling easily the non-convex parts (i.e. eye holes) with low shape distortion.

Table 1: Appraisal of time complexity of Mesh Parameterization algorithms.  $c$  denotes the number of iterations before convergence for that particular algorithm while  $|\partial M|$  denotes the number of vertices at the boundary of  $M$ .

Reference	Algorithm	Complexity
N/A	Our algorithm	$O(c \cdot n)$
(Donoho and Grimes, 2003)	Classic HLLC	$O(c \cdot n)$
(Floater, 1997)	Floater Parameterization	$O(c \cdot n)$
(Yoshizawa et al., 2004)	Stretch Minimizing Parameterization	$O(c_1 \cdot c_2 \cdot n)$
(Desbrun et al., 2002)	Intrinsic Parameterization	$O(c \cdot n)$
(Lévy et al., 2002)	LSCM	$O(c \cdot n)$
(Lee et al., 2002)	Virtual Boundary Parameterization	$O(c_1 \cdot n + c_2 \cdot  \partial M )$
(Zayer et al., 2007)	LinearABF	$O(c \cdot n)$
(Liu et al., 2008)	ASAP	$O(c \cdot n)$
(Liu et al., 2008)	ARAP	$O(c_1 \cdot c_2 \cdot n + c_3 \cdot  \partial M )$
(Sheffer and de Sturler, 2001)	ABF	$O(c_1 \cdot c_2 \cdot n)$
(Kharevych et al., 2006)	Discrete Conformal Mappings	$O(c_1 \cdot c_2 \cdot n)$
(Smith and Schaefer, 2015)	Free Boundary Parameterization	$O(c \cdot (n +  \partial M ))$



(a) High Frequency - High Curvature dataset.



(b) Non-bijective parameterization of the High Frequency - High Curvature dataset with our algorithm.

Figure 8: Failure test for our algorithm.

## 4.2 Time Complexity Comparison

In order to compare our algorithm with other Mesh Parameterization algorithms, table 1 presents an appraisal of the time complexity of several Mesh Parameterization algorithms. Classic HLLC and our algorithm compute the first three eigenvectors of the Hessian estimator by the Implicitly Restarted Lanczos



Figure 9: Texture map on the Face dataset computed with our algorithm.

Method with time complexity  $O(c \cdot n)$  (here we denote  $c \geq 1$  as the number of iterations executed by the algorithm before convergence). Other Mesh Parameterization algorithms rely on solving a linear system of equations, which is usually solved by a Conjugate (or Bi-Conjugate) Gradient Method once ( $O(c \cdot n)$ ) or several times ( $O(c_1 \cdot c_2 \cdot n)$ ). It is important to note that  $c$  is not the same between algorithms, but it is stated that such number is relatively low in applications after matrix preconditioning as well as use of initial parameterizations in iterative algorithms.

## 5 CONCLUSIONS

This article presents a variation of the classic HLLC algorithm for parameterization of triangular meshes. Classic HLLC was selected for this purpose since it has shown experimentally better results than other DR algorithms for Mesh Parameterization. An intuitive approach from Differential Geometry is followed by estimating locally the tangent Hessian with quadratic

interpolation and computing a partition of unity for the triangular mesh  $M$  as opposed to classic HLLÉ approach. In addition, each local parameterization is achieved by projecting onto the local average triangle normals plane instead of the usual PCA, which reflects better the local geometry of the surface specially in cases of sharp features.

The *Brain* dataset was parameterized with both Classic HLLÉ and our algorithm resulting in a higher rate of success (96.63%) for our approach against classic HLLÉ (76.40%). The *Face* dataset was also considered, resulting in a bijective parameterization with low shape distortion despite having holes. Complexity analysis showed that our algorithm asymptotically behaves similar to Mesh Parameterization algorithms that rely on solving a linear system of equations only once.

## 5.1 Ongoing Work

Segmentation of complex meshes with high gaussian curvatures into smaller ones increases the probability of finding bijective parameterizations. Therefore, automatic mesh segmentation for this task becomes crucial for parameterization of large and complex datasets.

## ACKNOWLEDGEMENTS

This research has been funded by the Research Group and College of Engineering at Universidad EAFIT, Colombia.

## REFERENCES

- Athanasiadis, T., Zioupos, G., and Fudos, I. (2013). Efficient computation of constrained parameterizations on parallel platforms. *Computers & Graphics*, 37(6):596–607. Shape Modeling International (SMI) Conference 2013.
- Belkin, M. and Niyogi, P. (2003). Laplacian eigenmaps for dimensionality reduction and data representation. *Neural Computation*, 15(6):1373–1396.
- Desbrun, M., Meyer, M., and Alliez, P. (2002). Intrinsic parameterizations of surface meshes. *Computer Graphics Forum*, 21(3):209–218.
- Desikan, R. S., Ségonne, F., Fischl, B., Quinn, B. T., B. C. D., Blacker, D., Buckner, R. L., Dale, A. M., Maguire, R. P., Hyman, B. T., Albert, M. S., and Killiany, R. J. (2006). An automated labeling system for subdividing the human cerebral cortex on +mri scans into gyral based regions of interest. *NeuroImage*, 31(3):968–980.
- Donoho, D. L. and Grimes, C. (2003). Hessian eigenmaps: Locally linear embedding techniques for high-dimensional data. *Proceedings of the National Academy of Sciences*, 100(10):5591–5596.
- Floater, M. S. (1997). Parametrization and smooth approximation of surface triangulations. *Computer Aided Geometric Design*, 14(3):231–250.
- Kharevych, L., Springborn, B., and Schröder, P. (2006). Discrete conformal mappings via circle patterns. *ACM Transactions on Graphics*, 25(2):412–438.
- Lafon, S. and Lee, A. (2006). Diffusion maps and coarse-graining: a unified framework for dimensionality reduction, graph partitioning, and data set parameterization. *Pattern Analysis and Machine Intelligence, IEEE Transactions on*, 28(9):1393–1403.
- Lee, Y., Kim, H. S., and Lee, S. (2002). Mesh parameterization with a virtual boundary. *Computers & Graphics*, 26(5):677–686.
- Lévy, B., Petitjean, S., Ray, N., and Maillot, J. (2002). Least squares conformal maps for automatic texture atlas generation. In ACM, editor, *ACM SIGGRAPH conference proceedings*.
- Liu, L., Zhang, L., Xu, Y., Gotsman, C., and Gortler, S. J. (2008). A local/global approach to mesh parameterization. In *Proceedings of the Symposium on Geometry Processing, SGP '08*, pages 1495–1504, Aire-la-Ville, Switzerland, Switzerland. Eurographics Association.
- Roweis, S. T. and Saul, L. K. (2000). Nonlinear dimensionality reduction by locally linear embedding. *Science*, 290(5500):2323–2326.
- Ruiz, O. E., Mejia, D., and Cadavid, C. A. (2015). Triangular mesh parameterization with trimmed surfaces. *International Journal on Interactive Design and Manufacturing (IJIDeM)*, pages 1–14.
- Sheffer, A. and de Sturler, E. (2001). Parameterization of faceted surfaces for meshing using angle-based flattening. *Engineering with Computers*, 17(3):326–337.
- Smith, J. and Schaefer, S. (2015). Bijective parameterization with free boundaries. *ACM Transactions on Graphics*, 34(4):70:1–70:9.
- Sun, X. and Hancock, E. R. (2008). Quasi-isometric parameterization for texture mapping. *Pattern Recognition*, 41(5):1732–1743.
- Tenenbaum, J. B., de Silva, V., and Langford, J. C. (2000). A global geometric framework for nonlinear dimensionality reduction. *Science*, 290(5500):2319–2323.
- Yoshizawa, S., Belyaev, A., and Seidel, H.-P. (2004). A fast and simple stretch-minimizing mesh parameterization. In *Shape Modeling Applications, 2004. Proceedings*, pages 200–208.
- Zayer, R., Lévy, B., and Seidel, H.-P. (2007). Linear angle based parameterization. In *ACM/EG Symposium on Geometry Processing conference proceedings*.
- Zhang, Z. and Zha, H. (2002). Principal manifolds and nonlinear dimension reduction via local tangent space alignment. *SIAM Journal of Scientific Computing*, 26:313–338.